

# BO Ari Light Curve Analysis using Ground-Based and TESS Data

Atila Poro<sup>1</sup>, Shiva Zamanpour<sup>1</sup>, Maryam Hashemi<sup>1</sup>, Yasemin Aladağ<sup>3</sup>, Nazim Aksaker<sup>2,3</sup>, Samaneh Rezaei<sup>1</sup>, Arif Solmaz<sup>3</sup>

<sup>1</sup>The International Occultation Timing Association Middle East section, Iran, info@iota-me.com

<sup>2</sup>Adana Organised Industrial Zones Vocational School of Technical Science, University of Çukurova, 01410, Adana, Turkey

<sup>3</sup>Space Science and Solar Energy Research and Application Center (UZAYMER), University of Çukurova, 01330, Adana, Turkey

## ABSTRACT

We present new BVR band photometric light curves of BO Arias obtained in 2020 and combined them with the Transiting Exoplanet Survey Satellite (TESS) light curves. We obtained times of minima based on Gaussian and Cauchy distributions and then applied the Monte Carlo Markov Chain (MCMC) method to measure the amount of uncertainty from our CCD photometry and TESS data. A new ephemeris of the binary system was computed employing 204 times of minimum. The light curves were analyzed using the Wilson-Devinney binary code combined with the Monte Carlo (MC) simulation. For this light curve solution, we considered a dark spot on the primary component. We conclude that this binary is an A-type system with a mass ratio of  $q = 0.2074 \pm 0.0001$ , an orbital inclination of  $i = 82.18 \pm 0.02$  deg, and a fillout factor of  $f = 75.7 \pm 0.8\%$ . Our results for the  $a$  ( $R_{\odot}$ ) and  $q$  parameters are consistent with the results of the Xu-Dong Zhang and Sheng-Bang Qian (2020) model. The absolute parameters of the two components were calculated and the distance estimate of the binary system was found to be  $142 \pm 9$  pc.

Keywords: Techniques: photometric; Stars: binaries: eclipsing; Stars: individual: BO Ari

## 1. INTRODUCTION

EW-type binaries are systems with main characteristics such as fairly equal depth eclipsing light curves, short orbital periods, less than one day, and frequently mass transfer between the two components which are in contact with each other sharing a common convective envelope. Eclipsing binaries can provide fundamental stellar properties and critical tests on the theories of stellar evolution and structure (Yuan et al. 2019).

Nicholson and Varley (2006) discovered the short-period binary system BO Ari (ASAS J021208+2708.2) and determined the first orbital period of  $0.3182^d$ . It was later observed by Acerbi et al. (2011) and classified as an A-type W Ursae Majoris system with a mass ratio of  $q = 0.1889$  and contact degree of  $f = 58.7\%$ . Gürol et al. (2015) made the first Spectroscopic observations and derived the  $q = 0.19024$  and  $f = 49.8\%$  by combining a light and radial velocity curve solution. Through the BVR observations done by Kriwattanawong et al. (2016) a mass ratio of  $q = 0.1754$  and contact degree of  $f = 27.72\%$  were obtained for the binary system.

In this study, the multi-color CCD light curves in  $B$ ,  $V$ , and  $R$  bands along with photometric data obtained from the TESS are presented. We determined a new ephemeris for this binary system. The light curve solution with Wilson-Devinney code combined with the MC simulation was performed to obtain reliable photometric parameters. Absolute parameters and distance of the system were derived.

## 2. NEW PHOTOMETRIC OBSERVATION

The observation of BO Ari was carried out by a 50 cm Ritchey-Chretien RC 500/4000 Pro RC SGA OTA telescope and Apogee Aspen CG6 LN-2-G07-S58 type CCD during nine nights of observation at the UZAYMER Observatory, Çukurova University, Adana, Turkey in January 2020. The CCD has a  $1024 \times 1024$  pixel array with a pixel length of  $24\mu$ . In these observation nights, we used the BVR standard Johnson filters for the photometry. Each of the frames was  $2 \times 2$  binned with 40s exposure time for  $R$  filter, 60s for  $V$  filter, and 90s for  $B$  filter; the average temperature of the CCD was  $-43^{\circ}\text{C}$  during the observations.

TYC 1761-2002-1, TYC 1761-1358-1, WISEA J021218.9 (NED), and WISEA J021158.5 (NED) were chosen as comparison stars, and BD+26 369 was selected as a check star. All of these stars are close to BO Ari and the

magnitude of the check star is appropriate. Figure 1 shows an observed field-of-view for BO Ari with the comparisons and check stars; The characteristics of these stars are shown in Table 1.

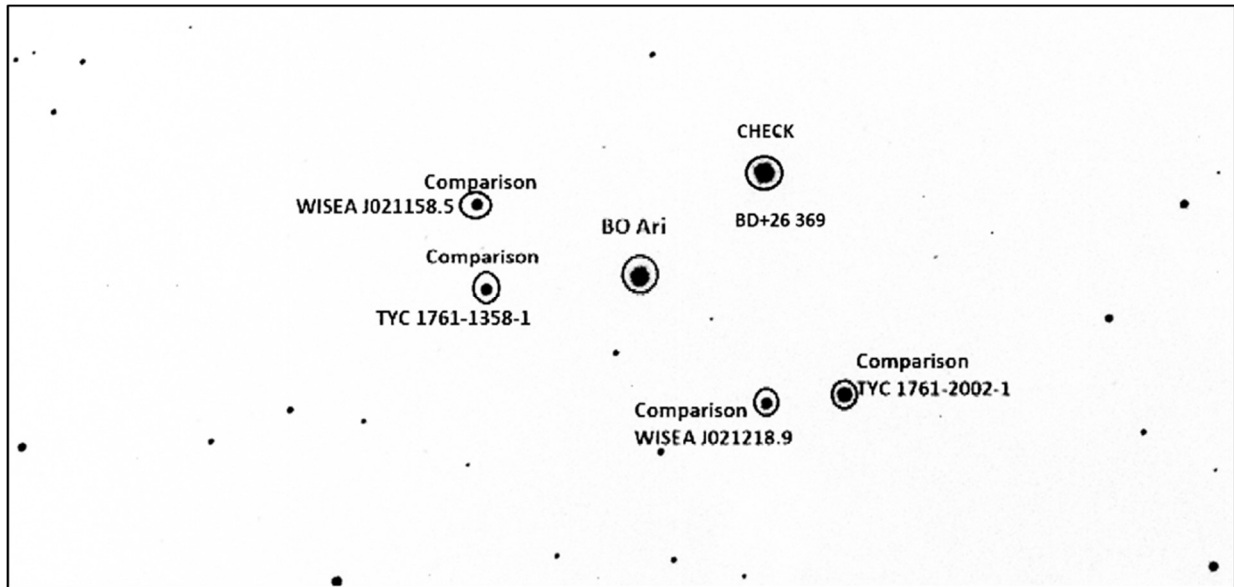


Figure 1. Observed field-of-view for BO Ari, comparison stars, and check star.

Table 1. Characteristics of the variable, comparison and check stars (from: Vizier-APASS9).

Star type	Star name	RA (J2000)	DEC (J2000)	Magnitude ( $V$ )
Variable	BO Ari	02 12 08.7070	+27 08 18.6180	10.169
Check	BD+26 369	02 12 11.1814	+27 10 19.8948	10.263
Comparison	TYC 1761-2002-1	02 12 22.4090	+27 08 33.4968	11.588
Comparison	TYC 1761-1358-1	02 12 01.7561	+27 07 03.1260	12.061
Comparison	WISEA J021218.9 (NED)	02 12 19.0166	+27 07 52.9630	12.780
Comparison	WISEA J021158.5 (NED)	02 11 58.5466	+27 07 53.1830	12.590

We reduced the raw CCD images and the basic data reduction was performed for bias, dark and flat-field according to the standard method. We aligned, reduced, and plotted raw images with AstrolmageJ (AIJ) software (Collins et al. 2017). AIJ provides an astronomy-specific image display environment and tools for astronomy-specific image calibration and data reduction. This software has been determined to identify the best linear fit of a dataset (by exerting air mass) to the light curve (Davoudi et al. 2020).

The study of eclipsing binaries has been advanced significantly with an increasing rate of discoveries as a result of space satellites. The Transiting Exoplanet Survey Satellite (TESS) is one of the recent missions that obtained new photometric observations data from numerous numbers of known eclipsing binaries. In this mission, the studied stars were 30 to 100 times brighter than those the Kepler mission and K2 follow-up surveyed, which enabled far easier follow-up observations with both ground-based and space-based telescopes. TESS also covered a sky area 400 times larger than that monitored by Kepler.

BO Ari (TIC 5674169) was observed by the TESS mission. TESS data of this binary system is available at the Mikulski Space Telescope Archive (MAST). We extracted TESS style curves using LightKurve code<sup>1</sup> from the MAST. It was observed in sector 18 by Camera 1 and CCD 3 in 120 seconds cadences. Its detrended light curves were extracted from the MAST.

### 3. NEW EPHEMERIS

<sup>1</sup><https://docs.lightkurve.org/>

Four primary and five secondary minimum times were determined from our observed light curves. They were found through fitting the models to the light curves and existing minima based on Gaussian and Cauchy distributions. We then employed the Monte Carlo Markov Chain (MCMC) method to measure the amount of uncertainty related to each value (Poro et al. 2020). We also benefited from Python along with its PyMC3 package to execute the lines of code (Salvatier et al. 2016). According to this method, we also calculated all times of minima of the TESS data for this binary system. Thus, 48 new times of minima were obtained from the TESS data.

Based on our observations, TESS data, and other literature we obtained 204 timings of minimum light including 98 primary and 106 secondary times of minima, given in Table 2.

We used the following reference ephemeris (Acerbi et al. 2011), for calculating epoch and O-C values,

$$BJD_{TDB} (Min. I) = 2452625.64163 + 0.3181963 \times E. \quad (1)$$

We fitted all mid-transit timings with a line, using the Robust regression and determined a new ephemeris for primary minimum as,

$$Min I (BJD_{TDB}) = (2452625.650338 \pm 0.001993) + (0.318194081 \pm 0.000000114) \times E \text{ days} \quad (2)$$

where  $E$  is an integer of orbital cycles after the reference epoch.

**Table 2. Times of minima of BO Ari.**

BJD <sub>TDB</sub> (Min.)	Error	Epoch	O-C	Reference	BJD <sub>TDB</sub> (Min.)	Error	Epoch	O-C	Reference
2451479.6573		-3601.5	-0.0004	Nicholson et al. 2006	2458798.7735	0.0002	19400.5	-0.0354	TESS
2452625.6416		0	0	Acerbi et al. 2011	2458798.9341	0.0001	19401	-0.0339	TESS
2454049.4086	0.0025	4474.5	-0.0024	Martignoni 2011	2458799.0918	0.0002	19401.5	-0.0353	TESS
2454062.4588		4515.5	0.0018	Acerbi et al. 2011	2458799.2523	0.0001	19402	-0.0339	TESS
2454080.4341		4572	-0.0010	Acerbi et al. 2011	2458799.4099	0.0002	19402.5	-0.0354	TESS
2454081.3885		4575	-0.0012	Acerbi et al. 2011	2458799.5706	0.0001	19403	-0.0338	TESS
2454083.2986		4581	-0.0003	Acerbi et al. 2011	2458799.7281	0.0002	19403.5	-0.0354	TESS
2454083.4591		4581.5	0.0011	Acerbi et al. 2011	2458799.8888	0.0001	19404	-0.0338	TESS
2454084.4135	0.0003	4584.5	0.0009	Martignoni 2011	2458800.0463	0.0002	19404.5	-0.0354	TESS
2454095.3901		4619	-0.0002	Acerbi et al. 2011	2458800.2071	0.0001	19405	-0.0337	TESS
2454507.2988	0.0100	5913.5	0.0033	Paschke 2009	2458800.3645	0.0002	19405.5	-0.0354	TESS
2454808.3048	0.0100	6859.5	-0.0043	Paschke 2009	2458800.5252	0.0001	19406	-0.0338	TESS
2455080.3633	0.0003	7714.5	-0.0037	Demircan et al. 2011	2458800.6827	0.0002	19406.5	-0.0354	TESS
2455080.5190	0.0001	7715	-0.0071	Gokay et al. 2010	2458800.8435	0.0001	19407	-0.0337	TESS
2455103.4287	0.0003	7787	-0.0075	Gokay et al. 2010	2458801.1164	0.0021	19408	-0.0790	TESS
2455103.5895	0.0004	7787.5	-0.0058	Gokay et al. 2010	2458801.0023	0.0003	19407.5	-0.0340	TESS
2455144.3197	0.0008	7915.5	-0.0047	Gokay et al. 2010	2458801.6384	0.0002	19409.5	-0.0343	TESS
2455392.5079	0.0001	8695.5	-0.0097	Demircan et al. 2011	2458801.7980	0.0001	19410	-0.0338	TESS
2455487.3302	0.0002	8993.5	-0.0099	Gokay et al. 2012	2458801.9552	0.0002	19410.5	-0.0357	TESS
2455487.4897	0.0001	8994	-0.0095	Gokay et al. 2012	2458802.1158	0.0002	19411	-0.0342	TESS
2455509.2849		9062.5	-0.0107	Gürol et al. 2015	2458803.5463	0.0002	19415.5	-0.0356	TESS
2455509.4448	0.0008	9063	-0.0099	Gokay et al. 2012	2458803.7071	0.0001	19416	-0.0339	TESS
2455528.3776		9122.5	-0.0098	Gokay et al. 2012	2458803.8645	0.0002	19416.5	-0.0356	TESS
2455538.2425		9153.5	-0.0090	Gürol et al. 2015	2458804.0254	0.0001	19417	-0.0338	TESS
2455551.2880	0.0001	9194.5	-0.0095	Gokay et al. 2012	2458804.1827	0.0002	19417.5	-0.0356	TESS
2455553.1970	0.0001	9200.5	-0.0097	Gokay et al. 2012	2458804.3435	0.0001	19418	-0.0339	TESS
2455553.3538		9201	-0.0120	Gürol et al. 2015	2458804.5009	0.0002	19418.5	-0.0356	TESS
2455887.1404		10250	-0.0133	Kriwattanawong 2016	2458804.6616	0.0001	19419	-0.0340	TESS
2455890.1630		10259.5	-0.0136	Kriwattanawong 2016	2458804.8192	0.0002	19419.5	-0.0355	TESS
2455890.3228		10260	-0.0129	Kriwattanawong 2016	2458804.9797	0.0001	19420	-0.0341	TESS
2455892.0724		10265.5	-0.0133	Kriwattanawong 2016	2458805.1373	0.0002	19420.5	-0.0356	TESS
2455892.2325		10266	-0.0123	Kriwattanawong 2016	2458805.2979	0.0001	19421	-0.0341	TESS
2456167.9468	0.0020	11132.5	-0.0151	Nelson 2013	2458805.4556	0.0002	19421.5	-0.0355	TESS
2456279.6330	0.0001	11483.5	-0.0158	Diethelm 2013	2458805.6159	0.0001	19422	-0.0343	TESS

2456514.9366	0.0002	12223	-0.0184	Nelson 2014	2458805.7738	0.0002	19422.5	-0.0355	TESS
2456516.5268		12228	-0.0192	Paschke 2014	2458805.9342	0.0001	19423	-0.0342	TESS
2456526.8689	0.0003	12260.5	-0.0185	Nelson 2014	2458806.0920	0.0002	19423.5	-0.0355	TESS
2456535.9372	0.0002	12289	-0.0188	Nelson 2014	2458806.2523	0.0001	19424	-0.0343	TESS
2456560.9153		12367.5	-0.0191	Nelson 2014	2458806.4102	0.0002	19424.5	-0.0355	TESS
2456579.6893	0.0002	12426.5	-0.0187	Nelson 2014	2458806.5705	0.0001	19425	-0.0343	TESS
2456579.8483	0.0002	12427	-0.0188	Nelson 2014	2458806.7284	0.0002	19425.5	-0.0355	TESS
2456630.2818	0.0025	12585.5	-0.0194	Hubscher 2014	2458806.8887	0.0001	19426	-0.0343	TESS
2456630.4414	0.0018	12586	-0.0189	Hubscher 2014	2458807.0465	0.0002	19426.5	-0.0356	TESS
2456928.7469	0.0002	13523.5	-0.0224	Nelson 2015	2458807.2069	0.0001	19427	-0.0343	TESS
2456949.1106		13587.5	-0.0233	Nagai 2015	2458807.3647	0.0002	19427.5	-0.0355	TESS
2456949.2708		13588	-0.0222	Nagai 2015	2458807.5250	0.0001	19428	-0.0343	TESS
2456978.3858	0.0014	13679.5	-0.0221	Hubscher 2015	2458807.6829	0.0002	19428.5	-0.0355	TESS
2456978.5435	0.0015	13680	-0.0235	Hubscher 2015	2458807.8432	0.0001	19429	-0.0343	TESS
2457329.3525		14782.5	-0.0259	Hubscher 2017	2458808.0012	0.0002	19429.5	-0.0354	TESS
2457329.5109		14783	-0.0266	Hubscher 2017	2458808.1614	0.0001	19430	-0.0343	TESS
2457329.6699		14783.5	-0.0267	Hubscher 2017	2458808.3193	0.0002	19430.5	-0.0355	TESS
2457758.2768		16130.5	-0.0302	Paschke 2017	2458808.4796	0.0001	19431	-0.0343	TESS
2458098.5868		17200	-0.0312	Nelson 2018	2458808.6375	0.0002	19431.5	-0.0355	TESS
2458380.5070	0.0001	18086	-0.0329	Ozavci et al. 2019	2458808.7977	0.0001	19432	-0.0344	TESS
2458790.8188	0.00016	19375.5	-0.0352	TESS	2458808.9558	0.0002	19432.5	-0.0354	TESS
2458790.9789	0.00013	19376	-0.0342	TESS	2458809.1159	0.0001	19433	-0.0344	TESS
2458791.4550	0.00017	19377.5	-0.0354	TESS	2458809.2739	0.0002	19433.5	-0.0355	TESS
2458791.6154	0.00013	19378	-0.0341	TESS	2458809.4340	0.0001	19434	-0.0345	TESS
2458791.7733	0.00017	19378.5	-0.0353	TESS	2458809.5923	0.0002	19434.5	-0.0353	TESS
2458791.9336	0.00013	19379	-0.0341	TESS	2458809.7521	0.0001	19435	-0.0346	TESS
2458792.0915	0.00017	19379.5	-0.0353	TESS	2458809.9105	0.0002	19435.5	-0.0353	TESS
2458792.2518	0.00012	19380	-0.0341	TESS	2458810.0702	0.0001	19436	-0.0347	TESS
2458792.4097	0.00017	19380.5	-0.0353	TESS	2458810.2288	0.0002	19436.5	-0.0352	TESS
2458792.5700	0.00013	19381	-0.0341	TESS	2458810.3883	0.0001	19437	-0.0348	TESS
2458792.7278	0.00017	19381.5	-0.0354	TESS	2458810.5470	0.0002	19437.5	-0.0352	TESS
2458792.8883	0.00013	19382	-0.0340	TESS	2458810.7065	0.0001	19438	-0.0348	TESS
2458793.0461	0.00017	19382.5	-0.0353	TESS	2458810.8653	0.0002	19438.5	-0.0351	TESS
2458793.2064	0.00013	19383	-0.0341	TESS	2458811.0246	0.0001	19439	-0.0349	TESS
2458793.3643	0.00017	19383.5	-0.0353	TESS	2458811.1836	0.0002	19439.5	-0.0350	TESS
2458793.5246	0.00013	19384	-0.0341	TESS	2458811.3427	0.0001	19440	-0.0350	TESS
2458793.6825	0.00017	19384.5	-0.0353	TESS	2458811.5019	0.0002	19440.5	-0.0349	TESS
2458793.8428	0.00013	19385	-0.0341	TESS	2458811.6608	0.0001	19441	-0.0351	TESS
2458794.0007	0.00017	19385.5	-0.0353	TESS	2458811.8202	0.0002	19441.5	-0.0348	TESS
2458794.1610	0.00013	19386	-0.0341	TESS	2458811.9789	0.0001	19442	-0.0352	TESS
2458794.3188	0.00017	19386.5	-0.0354	TESS	2458812.1384	0.0002	19442.5	-0.0348	TESS
2458794.4792	0.00013	19387	-0.0341	TESS	2458812.2970	0.0001	19443	-0.0353	TESS
2458794.6371	0.00017	19387.5	-0.0353	TESS	2458812.4569	0.0002	19443.5	-0.0345	TESS
2458794.7974	0.00013	19388	-0.0341	TESS	2458812.6151	0.0001	19444	-0.0354	TESS
2458794.9552	0.00016	19388.5	-0.0354	TESS	2458812.7748	0.0002	19444.5	-0.0348	TESS
2458795.1156	0.00013	19389	-0.0341	TESS	2458812.9334	0.0001	19445	-0.0353	TESS
2458795.2734	0.00017	19389.5	-0.0354	TESS	2458813.0931	0.0002	19445.5	-0.0347	TESS
2458795.4338	0.00013	19390	-0.0341	TESS	2458813.2514	0.0001	19446	-0.0355	TESS
2458795.5917	0.00017	19390.5	-0.0353	TESS	2458813.4112	0.0002	19446.5	-0.0348	TESS
2458795.7520	0.00013	19391	-0.0341	TESS	2458813.5697	0.0001	19447	-0.0354	TESS
2458795.9098	0.00017	19391.5	-0.0354	TESS	2458813.7294	0.0002	19447.5	-0.0348	TESS
2458796.0702	0.00013	19392	-0.0341	TESS	2458813.8879	0.0001	19448	-0.0354	TESS
2458796.2280	0.00017	19392.5	-0.0354	TESS	2458814.0477	0.0002	19448.5	-0.0347	TESS
2458796.3884	0.00013	19393	-0.0341	TESS	2458814.2058	0.0001	19449	-0.0357	TESS
2458796.5462	0.00017	19393.5	-0.0354	TESS	2458814.3659	0.0002	19449.5	-0.0347	TESS
2458796.7066	0.00013	19394	-0.0341	TESS	2458814.5240	0.0001	19450	-0.0357	TESS
2458796.8644	0.00017	19394.5	-0.0354	TESS	2458814.6842	0.0002	19450.5	-0.0346	TESS
2458797.0250	0.00013	19395	-0.0339	TESS	2458814.8422	0.0001	19451	-0.0357	TESS
2458797.1826	0.00017	19395.5	-0.0354	TESS	2458814.9411	0.0012	19451	0.0632	TESS
2458797.3431	0.0001	19396	-0.0340	TESS	2458863.3684	0.0002	19603.5	-0.0344	This study
2458797.5008	0.0002	19396.5	-0.0354	TESS	2458868.3005	0.0003	19619	-0.0343	This study
2458797.6613	0.0001	19397	-0.0340	TESS	2458871.1632	0.0005	19628	-0.0354	This study

2458797.8190	0.0002	19397.5	-0.0354	TESS	2458871.3220	0.0002	19628.5	-0.0357	This study
2458797.9794	0.0001	19398	-0.0341	TESS	2458873.2320	0.0003	19634.5	-0.0349	This study
2458798.1372	0.0002	19398.5	-0.0354	TESS	2458874.1871	0.0003	19637.5	-0.0344	This study
2458798.2976	0.0001	19399	-0.0341	TESS	2458874.3463	0.0002	19638	-0.0343	This study
2458798.4554	0.0002	19399.5	-0.0354	TESS	2458875.2993	0.0002	19641	-0.0359	This study
2458798.6159	0.0001	19400	-0.0339	TESS	2458880.2317	0.0002	19656.5	-0.0355	This study

#### 4. PHOTOMETRIC SOLUTIONS

The BVR light curves from our ground-based observations and TESS light curve were analyzed with the Wilson & Devinney (1971) code combined with Monte Carlo (MC) simulations. This method can accurately obtain parameters and their uncertainties. So we used this method to search mass ratio. The free parameters in MC simulation and their ranges are given in Table 3.

**Table 3. Free parameters and searching ranges in MC Simulations.**

Parameter	Value
$i$ (deg)	60-90
$T_2$ (K)	5000-6500
$\Omega_{1,2}$	1.5-9
$q = (m_2/m_1)$	0.1-6
$l_1$	1-12
Phase shift	-0.03-0.03
co-latitude (deg)	0-180
Longitude (deg)	0-360
Spot radius (deg)	1-90
$T_{spot}/T_1$	0.7-1

Based on our data and after calibrating (Høg et al. 2000), we calculated  $(B - V)_{BO\ Ari} = 0^m.573$ . As a result, according to Eker et al. (2020), the effective temperature of the primary component was found to be 5873 K. Thus, this temperature value is close to the value as the Gaia DR2 catalog (5874 K). As shown in Figure 2, the obtained temperature from derived  $(B - V)$  color for the primary component of BO Ari is also in an acceptable range with the method of Sekiguchi and Fukugita (2000).

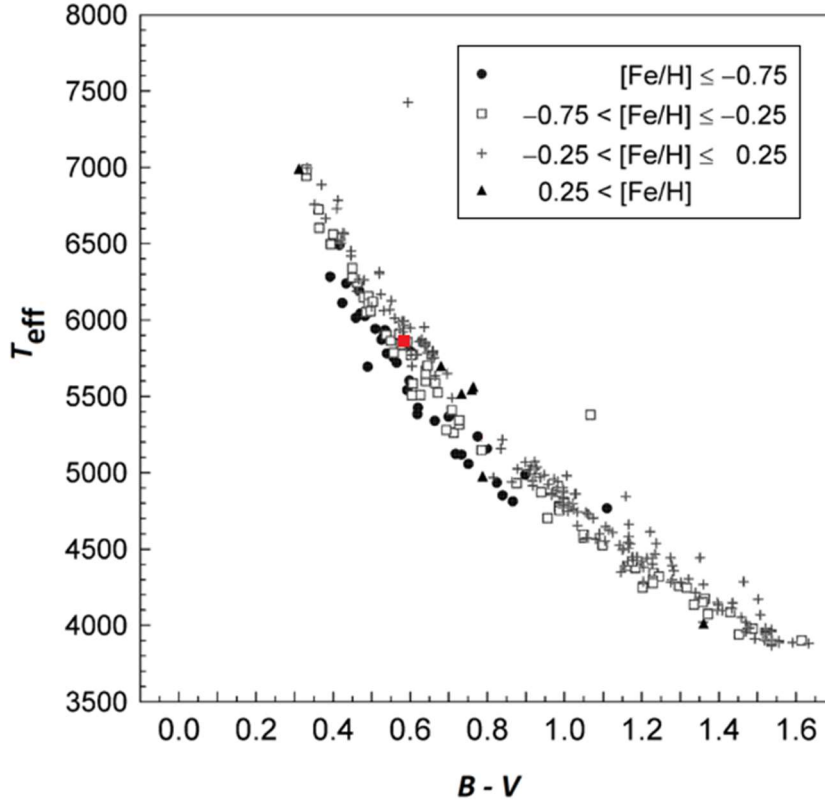


Figure 2. BO Ari's position (red dot) based on the Sekiguchi and Fukugita (2000) results.

The gravity-darkening coefficients  $g_1 = g_2 = 0.32$  (Lucy 1967) and bolometric albedo values  $A_1 = A_2 = 0.5$  (Rucinski 1969) were used, which correspond to the convective envelopes of both components. We assumed linear limb darkening coefficients taken from the tables published by Van Hamme (1993). The resulted parameter values obtained in the analysis of the light curves of BO Ari are given in Table 4, and the synthetic light curves based on these parameters are given in Figures 3 and 4.

Table 4. Photometric solutions of BQ Ari.

Parameter	Results
$T_1$ (K)	5873
$T_2$ (K)	5850(35)
$\Omega_1 = \Omega_2$	2.151(2)
$i$ (deg)	82.18(2)
$q$	0.2074(1)
$l_1/l_{tot}(B)$	0.7815(6)
$l_2/l_{tot}(B)$	0.2185(4)
$l_1/l_{tot}(V)$	0.7818(6)
$l_2/l_{tot}(V)$	0.2182(4)
$l_1/l_{tot}(R)$	0.7818(6)
$l_2/l_{tot}(R)$	0.2182(4)
$A_1 = A_2$	0.50
$g_1 = g_2$	0.32
$f$ (%)	75.7(8)
$r_1$ (back)	0.593(5)
$r_1$ (side)	0.562(4)
$r_1$ (pole)	0.508(4)

$r_2(\text{back})$	0.353(4)
$r_2(\text{side})$	0.278(3)
$r_2(\text{pole})$	0.263(3)
$r_1(\text{mean})$	0.553(2)
$r_2(\text{mean})$	0.295(4)
Colatitude <sub>spot</sub> (deg)	107(2)
Longitude <sub>spot</sub> (deg)	81(1)
Radius <sub>spot</sub> (deg)	21(1)
$T_{\text{spot}}/T_{\text{star}}$	0.92(2)
Phase Shift	0.01(1)

Notes: Parameters of a star spot on the primary component.

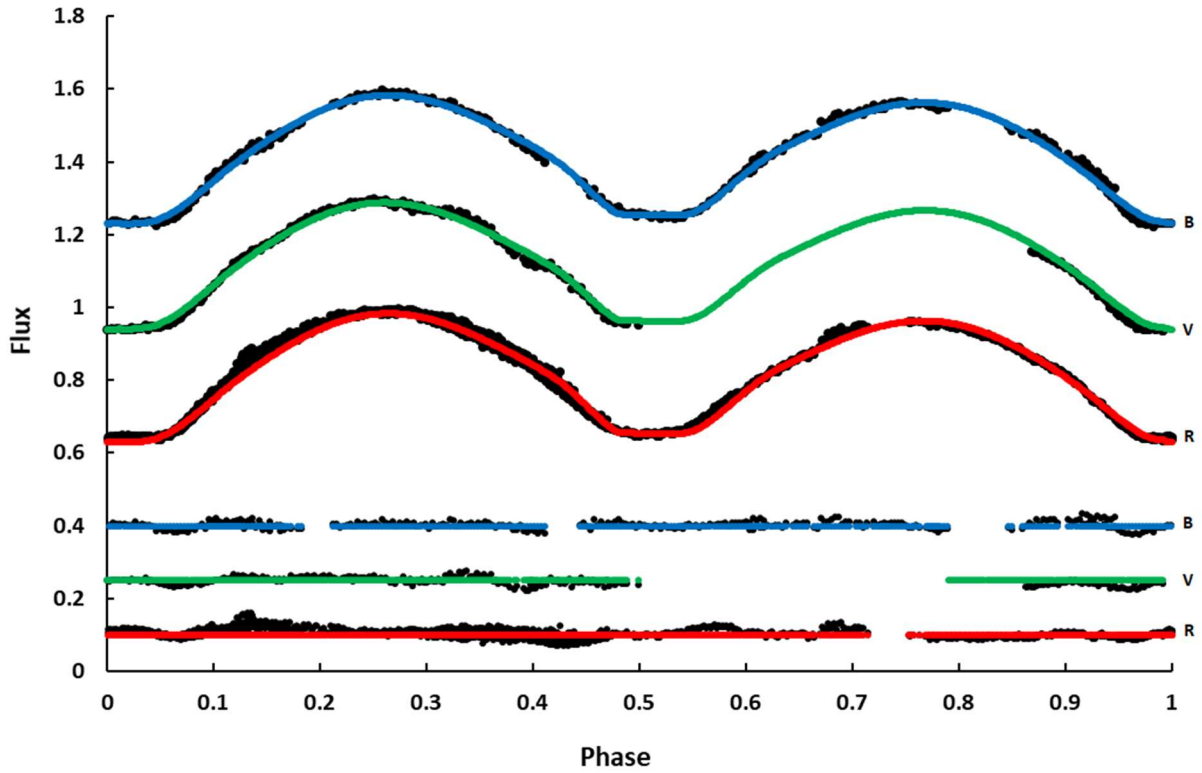


Figure 3. The observed light curves of BO Ari (black dots), and synthetic light curves obtained from light curve solutions in the *B*, *V*, and *R* filters (top to bottom respectively) and residuals are plotted; with respect to orbital phase, shifted arbitrarily in the relative flux.

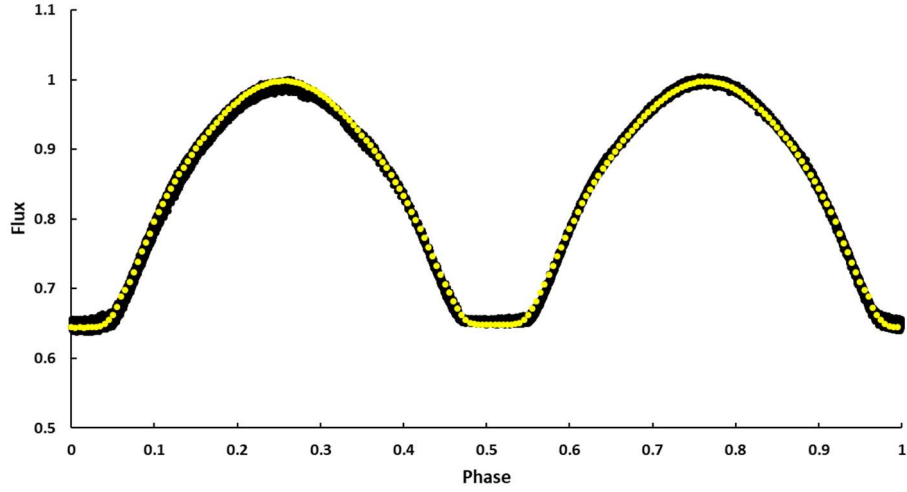


Figure 4. TESS observation and synthetic light curves of BO Ari.

The radial velocity of BO Ari is not available in this study, and we just can estimate the absolute parameters (Table 5). Accordingly, the mass of the primary component is derived from the Eker et al. (2020) study, and the mass of the secondary component was calculated from the equation  $q = \frac{m_2}{m_1}$ .

Table 5. Estimated absolute elements of BO Ari.

Parameter	Primary	Secondary
Mass ( $M_{\odot}$ )	1.095	0.227(15)
Radius ( $R_{\odot}$ )	1.190(7)	0.636(9)
Luminosity ( $L_{\odot}$ )	1.517(15)	0.425(11)
$M_{bol}$ (mag)	4.29(28)	5.67(23)
$\log g$ (cgs)	4.326(16)	4.187(13)
$a$ ( $R_{\odot}$ )	2.152(18)	

The 3D view and the geometrical structure of BO Ari is shown in Figure 5.

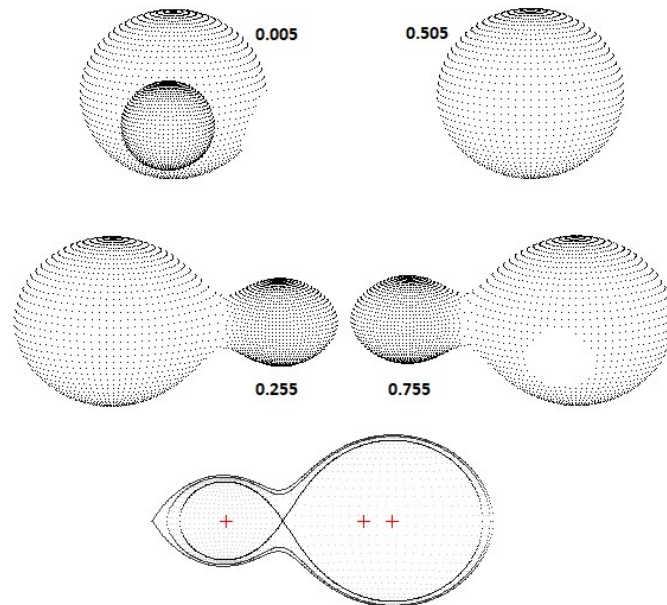


Figure 5. The positions of the components of BO Ari.



We estimated the binary system distance using the results of absolute parameters. The value of  $m_v = 10.14 \pm 0.005$  was calculated from the observational light curve, and  $M_v = 4.287 \pm 0.03$  was obtained using  $BC_1 = 0.003$  according to the Eker et al. (2020). Based on these values, we calculated the binary system's distance to be  $142 \pm 9$  pc, using  $A_{dv} = 0.09 \pm 0.02$  (Schlafly and Finkbeiner 2011).

## 5. CONCLUSIONS

We obtained the temperature of the primary component as  $T = 5873$  K by using  $B - V$ . This value is very close to the Gaia DR2's temperate for BO Ari which is  $T = 5874$ . It is found that BO Ari is a contact binary with a mass ratio of  $q = 0.2074 \pm 0.0001$ , a fillout factor of  $f = 75.7 \pm 0.8\%$ , and an inclination of  $i = 82.18 \pm 0.02$  deg. As indicated by the light curve solution, a cool starspot is placed on the primary component.

In order to study the characteristics of W UMa contact binaries, Xu-Dong Zhang and Sheng-Bang Qian (2020) have presented  $a - P$ , and  $q - P$  relations (Equations 3 and 4)

$$a = 10.285 \times P + 0.00155 \quad (3)$$

$$\log_{10}(1 + q) = 3\log_{10}(10.285 \times P + 0.00155) - 2\log_{10}P - \log_{10}(\sqrt{5198 \times P + 2.097} - 1.481) \quad (4)$$

where  $q$  is the mass ratio,  $a$  is the separation between two components, and  $P$  is the orbital period in year unit. The boundaries of these relations were given as,

$$a_u = 11.587 \times P + 0.00132 \quad (5)$$

$$a_l = 9.972 \times P + 0.00132 \quad (6)$$

$$\log_{10}(1 + q)_u = 3\log_{10}(11.587 \times P + 0.00132) - 2\log_{10}P - \log_{10}(\sqrt{4021 \times P + 1.868} - 1.300) \quad (7)$$

$$\log_{10}(1 + q)_l = 3\log_{10}(9.972 \times P + 0.00132) - 2\log_{10}P - \log_{10}(\sqrt{2701 \times P - 0.967} + 0.104) \quad (8)$$

We have derived  $a$  and  $q$  by using the above equations for BO Ari. The results of calculations the Xu-Dong Zhang and Sheng-Bang Qian (2020) relations show that the value of  $a(R_\odot) = 2.256$  and its lower and upper limit are 2.149-2.451; Also, for the  $q$  parameter, the value 0.3983 was obtained and the lower and upper limit of 0.0309-0.9389 was estimated; For both of these parameters, our results from this study ( $a(R_\odot) = 2.152$ ,  $q = 0.2074$ ) are in consistent with them. We have shown our system in Figure 6 according to these relations.

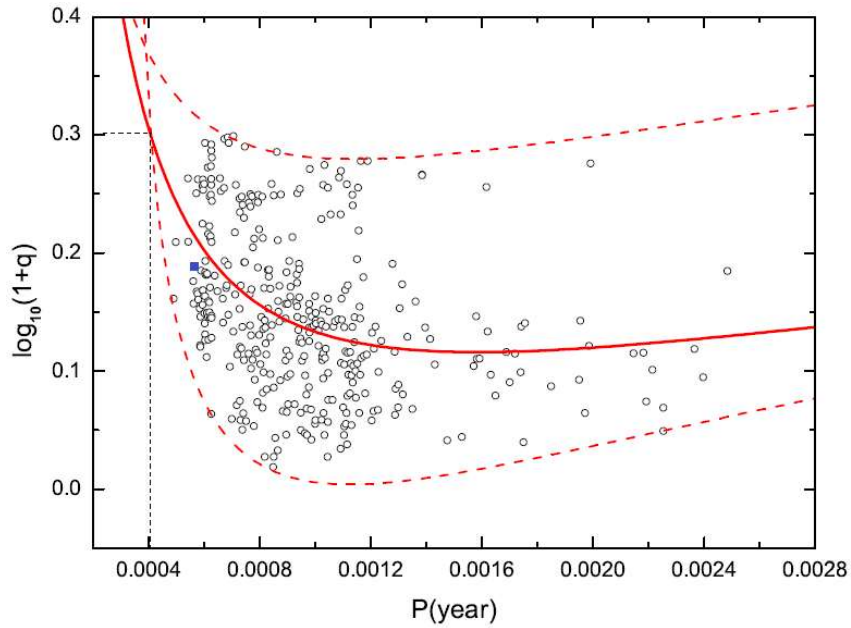


Figure 6. BO Ari's position based on the  $\log_{10}(1 + q) - P$  relation (blue dot). The suggested value for  $q$  (solid line) and the lower and upper limits for it (dotted line) are shown in the diagram.

We estimated the absolute parameters related to both components of BO Ari. Mass, radius, bolometric magnitude, and luminosity of the system were obtained. According to the estimated absolute parameters, we measured the distance as  $142 \pm 9$  pc. The Gaia EDR3 parallax gives a distance value of  $141.579 \pm 0.432$  pc. Therefore, our estimated distance for this binary system seems to be consistent with the Gaia EDR3 distance considering our estimated uncertainty.

The components' positions of BO Ari are plotted in the Hertzsprung-Russell (H-R) diagram and are shown in Figure 7, in which it seems the primary component is in the main-sequence, and the secondary component is placed near the ZAMS.

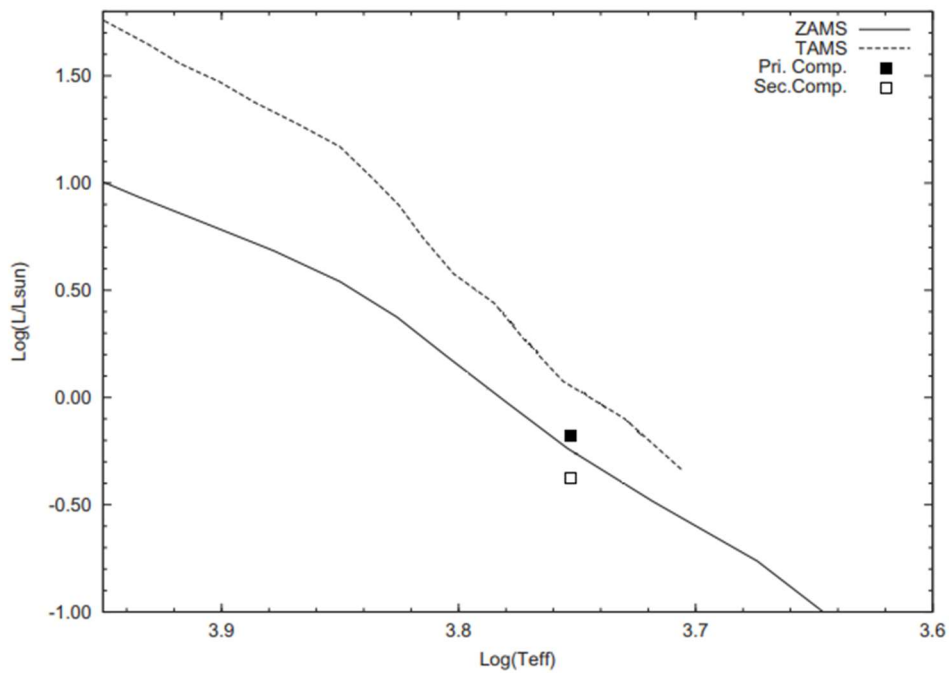


Figure 7. Position of both components of BO Ari on the H-R diagram, in which the theoretical ZAMS and TAMS curves are indicated.

According to the low mass ratio, a large of fillout factor, high inclination, and the very small temperature difference between components, we can conclude that BO Ari is an overcontact binary and A-type W UMa binary system. Given that the amount of evidence for a low mass ratio has increased from previous studies, we expect it will become deeper overcontact based on system evolution.

## ACKNOWLEDGEMENTS

This manuscript was prepared by a joint cooperation between the International Occultation Timing Association Middle East section (IOTA/ME) and Çukurova University, Adana, Turkey. We thank TÜBİTAK National Observatory for its support in providing the CCD to UZAYMER.

## References

- [1] Acerbi, F., Barani, C. and Martignoni, M., 2011. Photometric study and preliminary elements of the low-mass ratio W UMa system ASAS 021209+ 2708.3. *Research in Astronomy and Astrophysics*, 11(7), p.843.
- [2] Collins, K.A., Kielkopf, J.F., Stassun, K.G. and Hessman, F.V., 2017. AstrolmageJ: image processing and photometric extraction for ultra-precise astronomical light curves. *The Astronomical Journal*, 153(2), p.7
- [3] Davoudi F, Poro A, Alicavus F, Halavati A, Doostmohammadi S, A. Shahdadi A, et al. 2020. New Data on the Eclipsing Binary V1848 Ori and Improved Orbital and Light Curve Solutions. *Open Astron.* 29:72-80. DOI: <https://doi.org/10.1515/astro-2020-0013>.
- [4] Demircan, Y., Gurol, B., Gokay, G., Terzioglu, Z., Saral, G., Gursoytrak, H., Okan, A., Demirhan, U., Coker, D. and Derman, E., 2011. Minima times of some eclipsing binary stars. *IBVS*, 5965, p.2.
- [5] Diethelm, R., 2013. Timings of minima of eclipsing binaries. *IBVS*, 6042, p.2.
- [6] Eker, Z., Soydugan, F., Bilir, S., Bakis, V., Alicavus, F., Ozer, S., Aslan, G., Alpsoy, M. and Kose, Y., 2020. Empirical Bolometric Correction Coefficients for Nearby Main-Sequence Stars in Gaia Era. arXiv preprint arXiv:2006.01836.
- [7] Gokay, G., Demircan, Y., Gursoytrak, H., Terzioglu, Z., Okan, A., Dogruel, M.B., Saral, G., Cerit, S., Semuni, M., Kilic, Y. and Coker, D., 2012. Minima times of some eclipsing binary stars. *IBVS*, 6039, p.2.
- [8] Gokay, G., Demircan, Y., Terzioglu, Z., Gursoytrak, H., Okan, A., Coker, D., Saral, G., Gurol, B. and Derman, E., 2010. Minima Times of Some Eclipsing Binary Stars. *IBVS*, 5922, p.2.
- [9] Gürol, B., Gürsoytrak, S.H. and Bradstreet, D.H., 2015. Absolute and geometric parameters of contact binary BO Arietis. *New Astronomy*, 39, pp.9-18.
- [10] Hubscher, J., 2014. BAV Results of observations-photoelectric minima of selected eclipsing binaries and maxima of pulsating stars. *IBVS*, 6118, p.2.
- [11] Hubscher, J., 2015. BAV Results of observations-photoelectric minima of selected eclipsing binaries and maxima of pulsating stars. *IBVS*, 6152, p.2.
- [12] Hubscher, J., 2017. BAV Results of observations-photoelectric minima of selected eclipsing binaries and maxima of pulsating stars. *IBVS*, 6196, p.4.
- [13] Kriwattanawong, W., Tasuya, O. and Poojon, P., 2016. Period change investigation of the low mass ratio contact binary BO Ari. *New Astronomy*, 44, pp.12-16.
- [14] Lucy, L.B., 1967. Gravity-darkening for stars with convective envelopes. *Zeitschrift fur Astrophysik*, 65, p.89.
- [15] Martignoni, M., 2011. CCD Maxima of Pulsating Stars and Times of Minima of Eclipsing Binaries. *IBVS*, 6006, p.3.
- [16] Nagai, K., 2015. Visual, CCD and DSLR minima of eclipsing binaries during 2014. *VSOLJ*, 59, p.1.
- [17] Nelson, R.H., 2014. CCD Minima for Selected Eclipsing Binaries in 2013. *IBVS*, 6092, p.1.
- [18] Nelson, R.H., 2018. CCD Minima for Selected Eclipsing Binaries in 2017. *IBVS*, 6234, p.1.
- [19] Nelson, R.H., 2013. CCD Minima for Selected Eclipsing Binaries in 2012. *Information Bulletin of Variable Stars*, 6050, p.2.
- [20] Nelson, R.H., 2015. CCD Minima for Selected Eclipsing Binaries in 2014. *Information Bulletin on Variable Stars*, 6131, p.1.
- [21] Nicholson, M., Varley, H., 2006. Reports on new discoveries. *IBVS*, 5700, p.16.

- [22] Ozavci, I., Bahar, E., Izci, D.D., Ozuyar, D., Karadeniz, O., Sayar, B., Torun, S., Üzümcü, M., Azizoglu, B., Nasolo, Y. and Yilmaz, M., 2019. A list of minima times of some eclipsing binaries. *Open European Journal On Variable Stars*, p.2.
- [23] Paschke, A., 2014. A list of minima and maxima timings. *oejv*, 162, p.9.
- [24] Paschke, A., 2017. A list of minima and maxima timings. *oejv*, 181, p.6.
- [25] Paschke, A., 2009. A list of minima and maxima timings. *Open European Journal on Variable Stars*, (116), p.6.
- [26] Poro, A., Davoudi, F., Basturk, O., Esmer, E.M., Aksaker, N., Akyüz, A., Aladağ, Y., Rahimi, J., Lashgari, E., Ghanbarzadehchaleshtori, M. and Modarres, S., 2020. The First Light Curve Solutions and Period Study of BQ Ari. arXiv preprint arXiv:2006.00528.
- [27] Rucinski, S.M., 1969. The proximity effects in close binary systems. II. The bolometric reflection effect for stars with deep convective envelopes. *Acta Astronomica*, 19, p.245.
- [28] Salvatier, J., Wiecki, T.V. and Fonnesbeck, C., 2016. Probabilistic programming in Python using PyMC3. *PeerJ Computer Science*, 2, p.e55.
- [29] Schlafly, E.F. and Finkbeiner, D.P., 2011. Measuring reddening with Sloan Digital Sky Survey stellar spectra and recalibrating SFD. *The Astrophysical Journal*, 737(2), p.103. <https://doi.org/10.1088/0004-637X/737/2/103>.
- [30] Sekiguchi, M. and Fukugita, M., 2000. A Study of the B–V Color-Temperature Relation. *The Astronomical Journal*, 120(2), p.1072. <https://doi.org/10.1086/301490>.
- [31] Van Hamme, W., 1993. New limb-darkening coefficients for modeling binary star light curves. *The Astronomical Journal*, 106, pp.2096-2117.
- [32] Wilson, R.E. and Devinney, E.J., 1971. Realization of accurate close-binary light curves: application to MR Cygni. *The Astrophysical Journal*, 166, p.605.
- [33] Yuan, H.Y., Dai, H.F. and Yang, Y.G., 2019. IU Cancri: a solar-type contact binary with mass transfer. *Research in Astronomy and Astrophysics*, 19(6), p.085.
- [34] Zhang, X.D., and Qian, S.B., 2020. Orbital period cut-off of W UMa-type contact binaries. *Monthly Notices of the Royal Astronomical Society*, 497(3), pp.3493-3503. <https://doi.org/10.1093/mnras/staa2166>.